Bulgarian Chemical Communications, Volume 58, Issue 4 (pp. 461-475) 2026 *DOI: 10.34049/bcc.58.4.5746*

Gatifloxacin metal complexes: spectroscopic, thermal, and powder X-ray diffraction analysis with antimicrobial evaluation

M. Abu Sayeed[1,3], Md. Z. Sultan[2], M. Mehedi Masud[1], M. A. Rashid[1]*, H. Akhter Simol[2]

[1]*Department of Pharmaceutical Chemistry, Faculty of Pharmacy, University of Dhaka, Dhaka-1000, Bangladesh*

[2]*Centre for Advanced Research in Sciences (CARS), University of Dhaka, Dhaka-1000, Bangladesh*

[3]*Department of Pharmacy, Faculty of Science and Engineering, International Islamic University Chittagong, Kumira, Sitakunda, Chittagong-4318, Bangladesh*

Received: January 25, 2026; Revised: July 22, 2026

The rapid increase in antimicrobial resistance has compromised many antibiotics, highlighting the need for drug optimization. Metal complexation can improve antimicrobial agents' properties by enhancing activity and stability. Gatifloxacin readily forms complexes with various metal ions, potentially boosting its biological efficacy. Using specific transition and alkaline-earth metal ions, such as Mn(II), Sr(II), Co(II), Ca(II), Ni(II), Mg(II), Ba(II), Cu(II), Zn(II), Fe(II), Pb(II), and Ag(I), gatifloxacin-metal complexes were synthesized at a 1:1 molar ratio. Differential scanning calorimetry (DSC), Fourier transform infrared (FT-IR) spectroscopy, powder X-ray diffraction (PXRD), and microscopic examination were used to analyze the complexes to ascertain their thermal characteristics and coordination behavior. FT-IR spectral shifts together with DSC, PXRD, and microscopic observations suggested possible coordination of gatifloxacin with metal ions likely involving carboxylate and keto oxygen atoms. The synthesized complexes exhibited altered thermal and crystalline characteristics compared with free gatifloxacin. Disc-diffusion assays indicated that several complexes, particularly those of Cu(II), Co(II), Pb(II), Ag(I), Sr(II), and Mn(II), produced broader inhibition zones than free gatifloxacin against selected bacterial strains like *Bacillus tropicus, Salmonella typhi,* and *Streptococcus β-hemolyticus*. These findings provide preliminary evidence that metal complexation may influence the physicochemical and antibacterial properties of gatifloxacin. The results support metal complexation as a viable strategy for developing modified fluoroquinolone derivatives, subject to further confirmatory studies.

Keywords: antimicrobial activity, DSC, FT-IR, gatifloxacin-metal complexes, powder X-ray diffraction (PXRD).

INTRODUCTION

The alarming increase in antimicrobial resistance of antimicrobial drugs has arisen as a major global health threat, reducing the effectiveness of conventional antibiotics, and complicating the treatment of infectious diseases [1, 2]. Excessive and inappropriate antibiotic use has accelerated the evolution of resistant pathogens, emphasizing the urgent need to discover new antimicrobial agents or modify existing therapeutics to restore their clinical efficacy [3]. Among the various strategies explored, the design of drug-metal complexes has gained increasing attention, which may be related to their ability to enhance the physicochemical and biological properties of parent drugs [4-6]. Fluoroquinolones constitute an important class of synthetic broad-spectrum antibacterial agents that act primarily by inhibiting DNA gyrase and topoisomerase IV, enzymes essential for bacterial DNA replication [7, 8]. Structural modifications across different generations of fluoroquinolones have yielded compounds with improved potency, pharmacokinetics, and activity against resistant strains. Gatifloxacin, a fourth-generation fluoroquinolone, displays strong activity against both Gram-positive and Gram-negative bacteria and is widely used in respiratory, urinary tract and ocular infections (Fig. 1). Its molecular structure contains several potential donor sites—carboxylate, keto, methoxy and nitrogen atoms—capable of coordinating with transition and alkaline-earth metals to form stable chelate complexes [9, 10].

Chelation with metal ions is known to influence drug lipophilicity, membrane permeability, redox behavior, and overall biological activity. For fluoroquinolones, metal complexation often results in increased antibacterial potency may reflect reduced metal ion polarity, enhanced charge delocalization, and improved penetration of bacterial cell membranes.

* To whom all correspondence should be sent:
Email: *arpharm64@du.ac.bd*

© 2026 Bulgarian Academy of Sciences, Union of Chemists in Bulgaria

Numerous studies on ciprofloxacin-, norfloxacin-levofloxacin- and ofloxacin-metal complexes have demonstrated improved antibacterial activities compared to the free drugs. These results emphasize the potential of metal coordination as a valuable approach to develop more effective antimicrobial agents [11, 12].

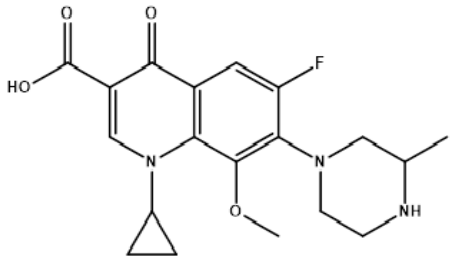


Figure 1. 2D structure of gatifloxacin (1-cyclopropyl-6-fluoro-8-methoxy-7-(3-methylpiperazin-1-yl)-4-oxoquinoline-3-carboxylic acid) which includes fluoroquinolone and quinolone.

As fluoroquinolone antibiotics contain several donor atoms that can chelate metal ions, drastically altering both their chemical properties and biological effects, it has been extensively studied. Coordination *via* the carboxylate and keto groups within the quinolone structure influences antibacterial efficacy and physicochemical characteristics, often enhancing activity relative to the unbound ligand, according to preliminary studies on the interactions between metals and fluoroquinolones. Antimicrobial resistance is a major worldwide problem that is driving research into new chemotherapeutic medicines and ways to improve the effectiveness of currently available antibiotics. Coordinating bioactive organic molecules with metal ions is a promising approach that frequently yields complexes with better physicochemical and biological characteristics than their original ligands [13]. Sultana *et al*. 's ground-breaking study showed the promise of gatifloxacin-metal complexes. They evaluated their antibacterial and immunomodulatory qualities and provided a thorough spectroscopic characterization. A broader spectrum of antimicrobial efficacy against both Gram-positive and Gram-negative organisms was demonstrated by some complexes, suggesting that complexation can affect biological responses in ways that go beyond simple bactericidal effects. This study provided preliminary evidence that complexation could change biological activity [14]. The investigations of Li *et al*. demonstrated the formation of gatifloxacin complexes with divalent metal ions and showed that these complexes exhibited more pronounced antibacterial effects against *Staphylococcus* strains than the parent antibiotic, indicating that complex formation may bring forth broader spectra of activity. Additionally, they reported the single-crystal X-ray structure of the bis(gatifloxacin) Cu(II) dihydrate complex [15]. Dave and Bhatt studied gatifloxacin compounds with alkaline earth metals (Mg(II), Ca(II), Sr(II), and Ba(II), going beyond transition metals. Before complexing with divalent metal ions, gatifloxacin was altered using auxiliary ligands such as o-phenylenediamine and 3-acetyl coumarin. According to their research, metal coordination may improve gatifloxacin derivatives' therapeutic potential [16]. Recently, Jawad *et al*. investigated complexes involving Sn(II) and Cd(II) ions. They observed increased inhibitory activity of specific complexes when compared to standard drugs [17]. Their results strengthen the idea that metal coordination influences biological activity and advocate for further investigation of these complexes as prospective antimicrobial agents. The review summarizes significant findings from recent research to provide context for the present study. Powder X-ray diffraction (PXRD) techniques remain one of the most powerful approaches for elucidating the structural properties of such complexes, as they provide insights into degree of crystallinity, lattice modifications, and emergence of new phases [18]. Drug-metal interactions can result in either stabilization of crystalline frameworks or partial amorphization, which directly influences drug performance in biological systems [19]. For example, fluoroquinolone antibiotics such as gatifloxacin and levofloxacin undergo significant structural modifications upon complexation with Mn(II) or Ba(II), often resulting in altered solubility and dissolution behavior [20].

Despite extensive data on other fluoroquinolones, reports on gatifloxacin-metal complexes remain relatively limited [21]. The few existing studies indicate that gatifloxacin can act as a bidentate ligand, coordinating typically through its carboxylate and keto oxygen atoms to form five- or six-membered chelate rings [22, 23]. Transition metal complexes of gatifloxacin have shown enhanced antibacterial activity, altered thermal properties and distinct coordination geometries. However, a comprehensive comparative evaluation of gatifloxacin complexes involving a broader range of biologically relevant metal ions is still lacking [24, 25]. In this context, the present work aims to synthesize, characterize, and evaluate the antimicrobial potential of gatifloxacin complexes formed with selected transition (Mn^{2+}, Co^{2+}, Ni^{2+}, Cu^{2+}, Zn^{2+}, Fe^{2+}) and alkaline earth/other metals (Ca^{2+}, Sr^{2+}, Mg^{2+}, Ba^{2+}, Pb^{2+}, Ag^{+}). Upon synthesis and characterization, their antimicrobial activities

were assessed against representative Gram-positive and Gram-negative pathogenic bacteria using the disc diffusion method. The present study provides a systematic comparison of gatifloxacin metal complexes, explores the influence of different metal ions on structural and biological properties, and identifies complexes with moderate to relatively strong antibacterial activity. The findings may support the development of metal-based antibiotic derivatives as promising candidates for addressing the growing challenge of antimicrobial resistance.

MATERIALS AND METHODOLOGY

Chemicals and reagents

Gatifloxacin (analytical grade) (potency 99.25%) was obtained as a kind gift from a reputable pharmaceutical company, Eskayef Pharmaceuticals Ltd., Dhaka, Bangladesh. Transition metal salts, including manganese(II) sulfate ($MnSO_4.H_2O$), strontium(II) chloride hexahydrate ($SrCl_2.6H_2O$), cobalt(II) nitrate hexahydrate [$Co(NO_3)_2.6H_2O$], calcium(II) carbonate ($CaCO_3$), nickel(II) sulfate hexahydrate ($NiSO_4.6H_2O$), magnesium(II) carbonate ($MgCO_3$), barium sulfate ($BaSO_4$), copper(II) sulfate pentahydrate ($CuSO_4.5H_2O$), zinc(II) sulfate monohydrate ($ZnSO_4.H_2O$), iron(II) sulfate heptahydrate ($FeSO_4.7H_2O$), magnesium(II) sulfate heptahydrate ($MgSO_4.7H_2O$), lead(II) nitrate [$Pb(NO_3)_2$] and silver(I) nitrate ($AgNO_3$) were procured from Merck, Germany. The analytical solutions were prepared using double-distilled water. All solvents, including ethanol, methanol, dimethyl sulfoxide (DMSO) and distilled water were of analytical grade.

Instruments

Differential scanning calorimeter (DSC) (model: DSC-60 WS, Shimadzu Corporation, Japan), FT-IR (IRTracer-100 type 8400S spectrometer, Shimadzu, Japan), trinocular microscope with camera (model: Olympus CKX-41), X-ray diffraction machine (model: RIGAKU Ultima IV X-ray diffractometer), fume hood (BFSD-201, Biolab Scientific, India), automatic digital autoclave (model: LS-50HD, manufactured by China & Origin Taisite, USA), laminar air flow bench (Wincom Company Ltd., China), heat-control stirring water bath (model: Unitronic OR, JP Selecta Company Spain), and round automatic autoclave steam sterilizer (LS-50HD, Nanbei Instrument Ltd, China) were used in the study.

Synthesis of gatifloxacin metal complexes

Gatifloxacin-metal complexes were synthesized *via* condensation of gatifloxacin with the selected metal salts individually to afford stable metal complexes. In a typical procedure, gatifloxacin was dissolved in methanol and pH was adjusted to ~6.8–7.2 to promote deprotonation of the carboxylic acid group [26]. The general procedure is as follows:

a) Preparation of metal salt solution: Thirteen single metal solutions were prepared at a 1 mMol concentration. Of each salt, an appropriate quantity was dissolved in 25-50 ml of methanol (90%)/ water (10%) under constant stirring.

b) Preparation of ligand solution: Gatifloxacin (1 mMol) was dissolved in a minimal volume of methanol (99%)/ DMSO (1%) under gentle heating to ensure complete dissolution. All the solutions prepared were filtered by using 0.45 μm membrane filter.

c) Complex formation: Drug solution was mixed individually with each salt solution at a millimolar ratio of 1:1, i.e., 25 ml of drug solution and 25 ml of salt solution.

d) Refluxing: The filtered mixtures were heated for 6.5 h at a temperature between 70 and 75 °C in a water bath under periodical stirring. Then the mixtures were left overnight in an oven at 100 °C for drying to get the complexes.

e) Isolation: The resulting precipitates were filtered, washed several times with ethanol and distilled water to remove unreacted ligand and metal salt, and dried under vacuum over silica gel.

f) Yield calculation: The percent yield of each complex was determined by weighing the dried product.

Characterization of metal complexes

The synthesized complexes were analyzed by studying the FT-IR spectra and the DSC thermograms. For FT-IR analysis discs were prepared by mixing potassium bromide with a metal-antibiotic complex in a 1:1 ratio. Thermal analysis of the test material was performed using a differential scanning calorimeter (DSC) to determine phase-transition temperatures (e.g., glass transition, melting) and associated enthalpy/heat-capacity changes. Samples of approximately 1–5 mg were accurately weighed into aluminum pans and sealed; an empty identical pan was used as the reference. The instrument was calibrated for temperature and heat flow using high-purity indium under the same experimental conditions. Measurements were conducted under inert nitrogen purge (e.g., 50 ml min^{-1}) to avoid oxidative artefacts. The temperature program consisted of initial isothermal hold at 25 °C for 5 min, followed by a linear heating ramp from 25 °C to 300 °C at 10 °C min^{-1}, then a cooling step to 25 °C and a second heating run under identical

conditions to erase previous thermal history. All heat-flow data were normalized to sample mass (W g^{-1}) and the onset, peak and area values of endothermic/exothermic transitions were reported. Baseline correction and peak integration were carried out using the instrument software, and each sample was run in duplicate to confirm reproducibility. Since elemental and magnetic investigations were not performed due to experimental constraints, the coordination behavior was inferred based on FT-IR and thermal data from FT-IR shifts and thermal behavior. X-ray diffraction studies were conducted using a Rigaku Ultima IV diffractometer equipped with Cu Kα radiation (λ = 1.5406 Å) over a 2θ range of 5–70° at a scanning rate of 3° min^{-1}. The PXRD patterns were recorded in the 2θ range of 5–70° at a scanning rate of 3°/min in continuous mode. The obtained diffraction data were compared to reference data from the International Centre for Diffraction Data (ICDD PDF-2 database, 2021) to identify crystalline phases [18]. The morphology and crystalline habit of the synthesized complexes were observed using a trinocular optical microscope. Images of drug-metal complexes were compared with the images of their parent drugs to assess morphological changes upon complexation.

Antimicrobial activity assessment

The following bacterial strains were used as clinical specimens: A) *Streptococcus β-hemolyticus*, B) *Staphylococcus aureus*, C) *Streptococcus pyogenes*, D) *Bacillus subtilis*, E) *Bacillus tropicus*, F) *Shigella dysenteriae*, G) *Klebsiella pneumoniae*, H) *Escherichia coli*, I) *Salmonella abony*, J) *Pseudomonas aeruginosa* and K) *Salmonella typhi* (Table 5). The antimicrobial effectiveness of the drug-metal complexes was evaluated using the disc diffusion method [27]. After preparing the nutrient agar, it was autoclaved for 21 min at 121 °C at atmospheric pressure, and then cooled to 45 °C. The media were then transferred into sterile Petri dishes and allowed to solidify. A sterile swab was used to inoculate the solidified media of each plate with the appropriate microbial suspension. A control disc and discs with the corresponding complexes were placed on the solidified media followed by incubation at 37 °C for 24 h. The diameters of the zones of inhibition surrounding the discs were measured and recorded in mm after the incubation period [28].

Statistical analysis

Each experiment was carried out in triplicate, and the mean diameters of the inhibitory zones were used to express the results.

RESULTS AND DISCUSSION

Synthesis and physical properties

Gatifloxacin metal complexes were synthesized by reacting gatifloxacin with transition and alkaline earth metal salts (Mn^{+2}, Sr^{+2}, Co^{+2}, Ca^{+2}, Ni^{+2}, Mg^{+2}, Ba^{+2}, Cu^{+2}, Zn^{+2}, Fe^{+2}, Pb^{+2}), and Ag^{+} in a 1:1 millimolar ratio. The synthesized complexes were analyzed using FT-IR spectroscopy and DSC. The physical properties along with the percentage yield of different salts, gatifloxacin (parent drug) and its metal complexes are shown in Tables 1 and 2. The color variations indicate successful coordination of the metal ions with gatifloxacin and are consistent with previous reports on fluoroquinolone metal complexes. Most of the complexes were sparingly soluble in water but soluble in DMSO and DMF, suggesting that influenced lipophilicity may reflect chelation [29].

FT-IR spectroscopy analysis

FT-IR spectra of the metal complexes revealed significant shifts in key functional group bands compared to free gatifloxacin. The carboxylic C=O stretching vibration, observed at ~1720 cm^{-1} in free gatifloxacin, shifted to 1716-1735 cm^{-1} in the complexes, indicating coordination through the carboxylate oxygen. Similarly, the quinolone C=O band at ~1625 cm^{-1} shifted to lower wavenumbers, consistent with possible involvement of the keto group in metal binding. New bands in the range 500–600 cm^{-1} were assigned to M–O and M–N vibrations, supporting the formation of metal–ligand bonds (Fig. 2). These observations suggest that gatifloxacin appears to behave coordinating *via* the carboxylate oxygen and ketone oxygen or piperazinyl nitrogen atoms, in line with previously reported bidentate coordination of fluoroquinolones *via* keto-carboxylate oxygen atoms, including norfloxacin, levofloxacin, and gemifloxacin [30, 31].

The formation of metal complexes and the coordination behavior of the ligand were investigated using FT-IR spectroscopy. The spectral data for the synthesized complexes were compared to infer the binding modes and is consistent with complexation. The key vibrational frequencies and their assignments are summarized in Table 3.

Table 1. Physical characteristics of gatifloxacin and metal salts

Sample	MW	Appearance/color	Solubility
Gatifloxacin	375.40	White to pale yellow	Water, DMSO and DMF
Manganese (II) sulfate monohydrate - $MnSO_4.H_2O$	169.00	Pale pink	Water
Strontium chloride hexahydrate - $SrCl_2.6H_2O$	266.62	White crystals	Water and alcohol
Cobalt (II) nitrate hexahydrate - $Co(NO_3)_2.6H_2O$	291.03	Red crystals	Water and alcohol
Calcium carbonate - $CaCO_3$	100.00	White powder	Methanol
Nickel (II) sulfate hexahydrate - $NiSO_4.6H_2O$	262.85	Green solid	Water
Magnesium carbonate - $MgCO_3$	84.32	White powder	Water
Barium sulfate - $BaSO_4$	233.38	White or yellowish odorless powder or small crystals	Water
Copper (II) sulfate pentahydrate - $CuSO_4.5H_2O$	249.69	Blue crystals or powder	Water
Zinc sulfate monohydrate - $ZnSO_4.H_2O$	179.45	White powder	Water
Iron (II) sulfate heptahydrate - $FeSO_4.7H_2O$	278.01	Green crystals	Water
Magnesium sulfate heptahydrate - $MgSO_4.7H_2O$	246.48	Colorless to white with pale shades of pink and green crystals	Water
Lead (II) nitrate-$Pb(NO_3)_2$	331.20	Colorless to white powder	Water
Silver nitrate ($AgNO_3$)	169.87	White crystal	Water

Table 2. Physical features of metal complexes of gatifloxacin with salts

Sample	Appearance/color	Solubility	% Yield
Manganese- gatifloxacin complex	Brown	DMSO and methanol	85
Strontium- gatifloxacin complex	Yellowish white	Water and methanol	81
Cobalt- gatifloxacin complex	pink	DMSO and methanol	75
Calcium - gatifloxacin complex	Off-whitish powder	Methanol	76
Nickel- gatifloxacin complex	Pale green solid	Methanol	75
Magnesium-gatifloxacin A complex*	White powder	Methanol, DMF	80
Barium- gatifloxacin complex	Yellowish-white powder	Methanol and DMSO	82
Copper (II) - gatifloxacin complex	Greenish-blue powder	Water	75
Zinc - gatifloxacin complex	White powder	DMSO	80
Iron (II) - gatifloxacin complex	Brown powder	DMF	75
Magnesium – gatifloxacin B complex*	White	Methanol	82
Lead - gatifloxacin complex	White powder	Water	85
Silver- gatifloxacin complex	Reddish-brown	Water, methanol	72

*Magnesium-gatifloxacin A and magnesium-gatifloxacin B complexes formed by interaction with magnesium carbonate- $MgCO_3$ and magnesium sulfate- $MgSO_4.7H_2O$, respectively.

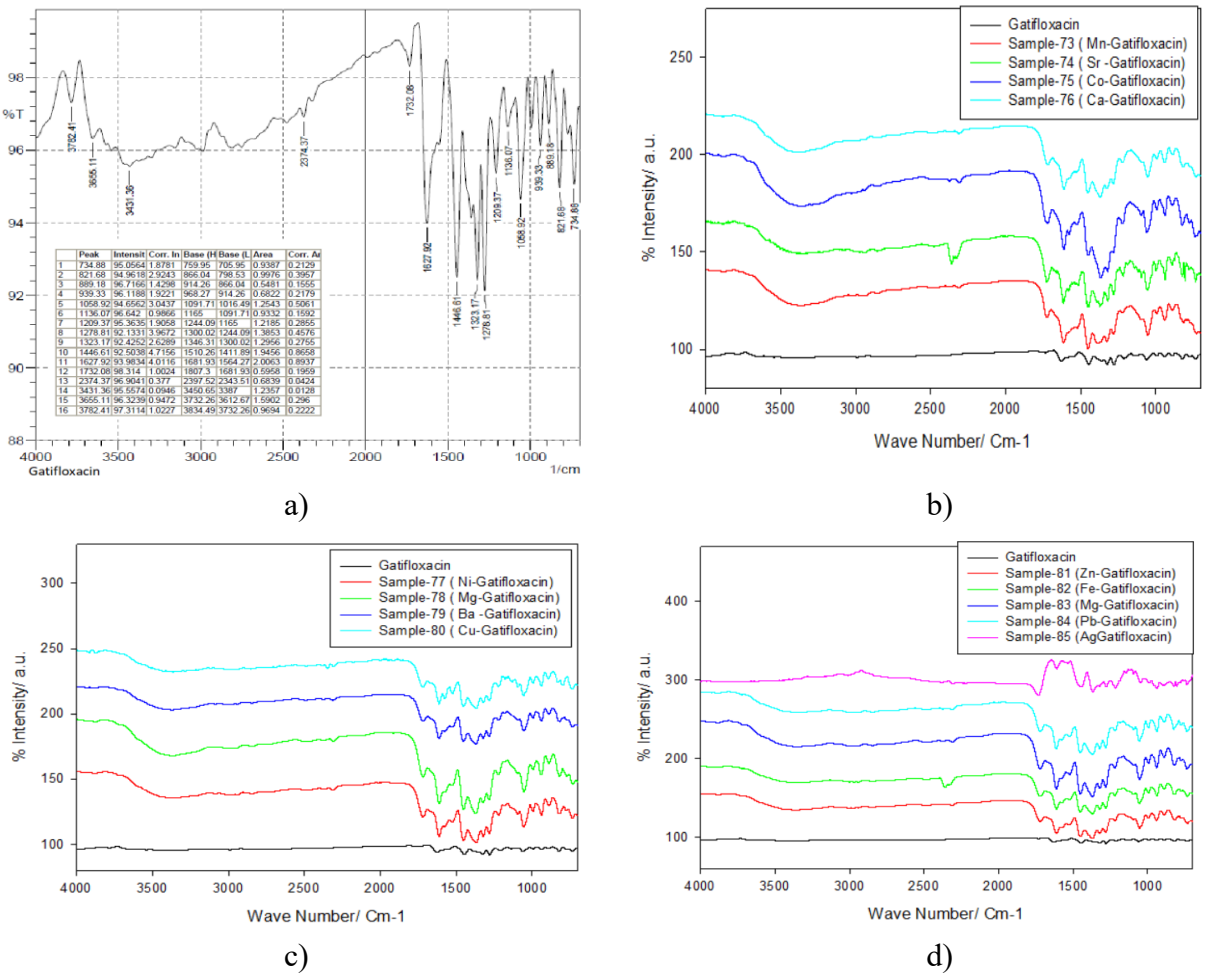


Figure 2. (a) FT-IR spectra of gatifloxacin; (b) Overlaying FT-IR spectra of gatifloxacin and complexes of Mn, Sr, Co and Ca; (c) Overlaying FT-IR spectra of gatifloxacin and complexes of Ni, Mg, Ba and Cu; (d) Overlaying FT-IR spectra of gatifloxacin and complexes of Zn, Fe, Mg, Pb and Ag.

Table 3. Characteristic FT-IR spectral data (cm^{-1}) for the synthesized complexes

Sample	Carboxylic /C=O stretch (Region I)	Quinolone /aromatic C=O (Region II)	M–O /M–N vibrations. 500-600 (New bands)
Manganese- gatifloxacin complex	1724.96	1625.66	Yes
Strontium- gatifloxacin complex	1726.29	1620.21	Yes
Cobalt- gatifloxacin complex	1720.5	1612.49	Yes
Calcium - gatifloxacin complex	1718.56, 1718.58	1622.49	Yes
Nickel- gatifloxacin complex	1716.66	1612.49	Yes
Magnesium- gatifloxacin A complex	1718.58	1610.56	Yes
Barium- gatifloxacin complex	1716.58	1610.56	Yes
Copper (II) - gatifloxacin complex	1716.86	1612.49	Yes
Zinc – gatifloxacin complex	1720.5	1610.56	Yes
Iron (II) - gatifloxacin complex	1720.5	1612.49	Yes
Magnesium - gatifloxacin B complex	1718.5	1610.56	Yes
Lead - gatifloxacin complex	1718.98	1612.49	Yes
Silver- gatifloxacin complex	1735.17	1609.62	Yes

The most significant evidence for complex formation is the shifting of key functional group vibrations associated with the ligand's potential donor atoms.

a) Carboxylate coordination: The stretching vibration for the carboxylic acid (C=O) group, which typically appears as a strong band above 1700 cm^{-1} in the free ligand, is observed in the range of approximately 1716-1727 cm^{-1} for most of the complexes. This shift, while present, is less pronounced than in some classical complexes, suggesting a specific coordination environment or hydrogen bonding network that influences the carbonyl frequency. A notable exception is the silver- gatifloxacin complex, which shows a distinct band at 1735 cm^{-1}, potentially indicating a different protonation state or weaker interaction with the metal center.

b) Ketone carbonyl coordination: A more consistent indication of possible coordination is the behavior of the quinolone ketone carbonyl band. In the spectra of the complexes, this vibration, which is expected near 1625 cm^{-1} for the free ligand, is systematically shifted to lower wavenumbers, appearing in the range of ~1610 - 1622 cm^{-1} across all complexes. This consistent redshift supports the possible involvement of the keto oxygen atom in coordination to the metal center.

c) Metal-ligand bond formation: The appearance of new, weak-to-medium intensity bands in the low-frequency region of 500-600 cm^{-1} (explicitly noted for the manganese-gatifloxacin complex) is a characteristic feature frequently associated with metal complexation. These bands are absent in the free ligand and are assigned to ν(M–O) and ν(M–N) vibrational modes, supporting the formation of coordinate covalent bonds between the metal ions and the ligand donor atoms. While not explicitly listed in every sample's peak table, the consistent shifts in the carbonyl regions imply the presence of these metal-ligand vibrations across the series.

The collective spectroscopic observations suggest with a possible bidentate coordination mode involving the carboxylate and keto oxygen atoms of gatifloxacin. However, without complementary techniques such as elemental analysis or magnetic susceptibility measurements, the exact coordination geometry (e.g., octahedral vs. tetrahedral) remains speculative. The structures in Fig. 3 are therefore proposed as plausible models rather than confirmed assignments.

The proposed structure of the metal–gatifloxacin complex shows bidentate coordination *via* the carboxylate and keto oxygen atoms, forming a six-membered chelate ring. M represents divalent metal ions. A suggested coordination structure for the gatifloxacin-metal complexes, shown in Fig. 3, is based on the shifts seen in the FT-IR spectra and is supported by previous research on fluoroquinolone-metal complexes.

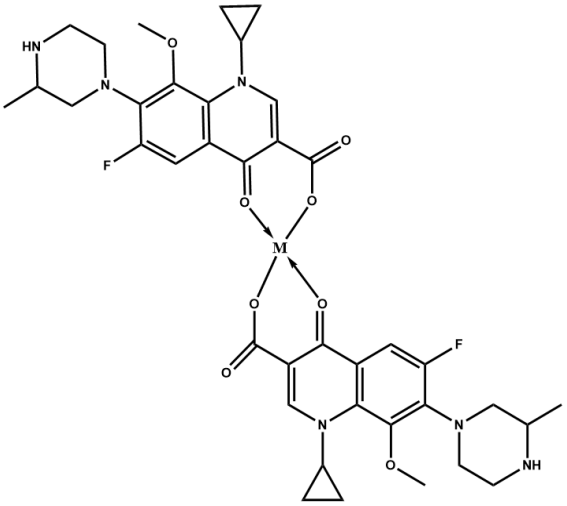


Figure 3. Plausible coordination model based on FT-IR, DSC, and PXRD observations together with previously reported fluoroquinolone coordination patterns.

By connecting through the oxygen atoms of the keto group at position 4 and the carboxylate group at position 3 of the quinolone ring, the ligand acts as a bidentate chelating agent. A stable six-membered chelate ring is formed with the metal ion because of this interaction. The complexes are anticipated to exhibit a proposed coordination mode, which is contingent upon the characteristics of the metal ion, and may necessitate further coordination with solvent molecules such as water. This suggested structure is consistent with fluoroquinolone antibiotic coordination modalities that have been previously reported.

The most plausible coordination mode involves the oxygen atoms of the carboxylate and the pyridone ketone group, forming a stable six-membered chelate ring with the metal center. This binding mode is consistent with the well-established coordination chemistry of fluoroquinolone antibiotics. The spectral variations observed across the formed complexes likely reflect subtle differences in the metal center, coordination geometry, or counterions, which can influence the precise vibrational frequencies. Apart from gatifloxacin, several fluoroquinolone antibiotics have been shown to act as bidentate ligands *via* the carboxylate ($–COO^–$) and keto (C=O) oxygen atoms. For instance, when norfloxacin forms stable chelate complexes with transition metal ions like Cu(II), Ni(II), and Zn(II), coordination occurs through the

3-carboxylate and 4-keto groups, resulting in the creation of six-membered chelate rings [10, 11]. Similarly, the FT-IR spectrum shifts, and the X-ray crystallographic investigations showed that levofloxacin coordinates with metal ions in a bidentate manner, indicating the involvement of the pyridone oxygen and carboxylate moiety [31, 32]. Similar coordination behavior is also shown in gemifloxacin, which forms stable metal complexes with enhanced biological activity when the ligand interacts with the quinolone core's oxygen donor atoms [29]. The coordination mode suggested for gatifloxacin in the current work is supported by these combined results, which demonstrate that bidentate coordination *via* keto-carboxylate groups is a distinguishing feature of fluoroquinolone drugs.

Differential scanning calorimetry (DSC) analysis

DSC thermograms of the pure drugs showed sharp endothermic peaks corresponding to their melting points, reflecting stability. Gatifloxacin exhibited a sharp melting transition around 190.13 °C. Based on the expanded DSC analysis of gatifloxacin-metal complexes, the Sr–gatifloxacin complex remains the most thermally stable one, exhibiting a significant endothermic event at 240.34 °C which is likely associated with melting or decomposition. In comparison, the Co–gatifloxacin complex shows a single thermal event at 138.19 °C, suggesting phase transition or dehydration. The Mn–gatifloxacin complex displays two mid-temperature events at 129.65 °C and 181.68 °C, which may correspond to successive dehydration steps or structural rearrangements. The Mg–gatifloxacin complex, with low-temperature events at 51.25 °C and 112.16 °C, appears to be the least stable, likely related to hydration or weaker metal coordination. Notably, the Ba–gatifloxacin complex shows no distinct thermal events up to 300 °C, indicating high thermal stability, possibly even higher than that of the Sr complex. These variations highlight the significant role of the metal ion in modulating the thermal behavior of gatifloxacin complexes, with larger metal ions like Sr^{2+} and Ba^{2+} conferring higher stability compared to transition metals like Mn^{2+} and Co^{2+}, or the smaller Mg^{2+} ion (Fig. 4). These variations in thermal behavior reflect the influence of the metal ion on the complex's crystallinity, stability, and hydration state, the Sr-complex being the most robust under thermal stress.

X-ray diffraction studies

The study of crystal structures of drug-metal complexes provides valuable insight into their stability, binding orientation, and physicochemical properties.

Metal ions often modulate the pharmacological activity of drugs through coordination, leading to altered solubility, crystallinity, and bioavailability. PXRD is one of the most powerful analytical techniques for characterizing crystalline phases, as it reveals both the molecular arrangement and the degree of order/disorder in solid-state materials. In this investigation, the crystalline structures of gatifloxacin-metal complexes were investigated using PXRD techniques.

- *Gatifloxacin and its Mn(II) complex*

The PXRD spectra for both pure gatifloxacin and its Mn(II) complex were obtained within a 2θ range of 5–70°. The pure gatifloxacin (form-Y) displayed distinct diffraction peaks at 2θ values of 5.1, 6.2, 7.8, 9.1, 9.8, 10.4, 12.9, 13.6, 14.3, 17.3, 17.7, 18.3, 18.8, 19.6, 20.7, 21.1, 23.4, 23.9, 24.4, 25.4, 25.9, and 26.6 ± 0.2°, which align with the previously documented crystalline data for gatifloxacin form-Y [33].

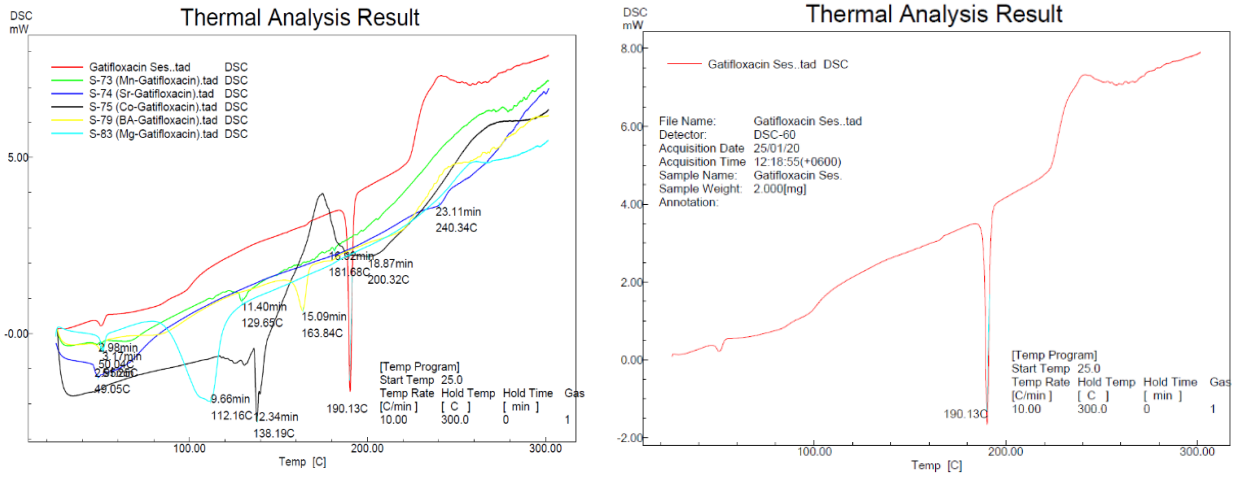


Figure 4. DSC spectra of different drug-metal complexes and gatifloxacin.

Upon interaction with $MnSO_4 \cdot H_2O$ (PDF Card No. 00-003-0370), the resulting diffractogram revealed additional peaks, alongside a decrease in intensity, broadening of peaks, and an increase in background noise when compared to pure gatifloxacin (https://trea.com/information/crystalline-forms-of-gatifloxacin/patentgrant/7a18a46e-c8f3-45ca-aea1-d4dccf0bdec6, accessed on 25th August 2025). These findings may suggest a partial disruption of the original crystalline lattice and the emergence of mixed amorphous–crystalline domains. Variations in peak position, intensity, and the appearance or disappearance of peaks in relation to the parent materials further imply the development of a modified crystalline phase or a change in solid-state organization following interaction with Mn(II) (Fig. 5).

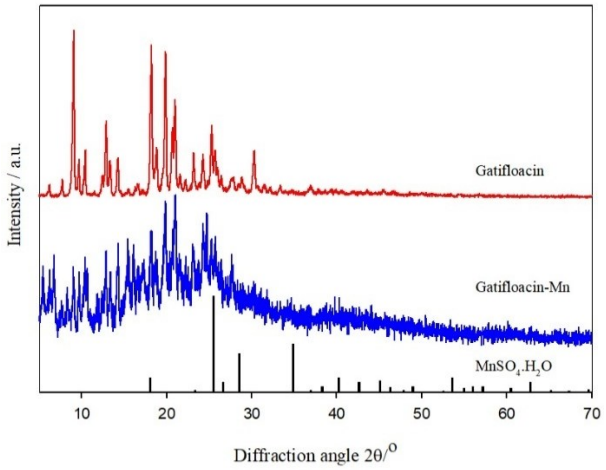


Figure 5. PXRD pattern of gatifloxacin-Mn complex.

- *Gatifloxacin and its Ba(II) complex*

Fig. 6 shows the PXRD pattern of (i) gatifloxacin and (ii) the gatifloxacin-Ba complex. The PXRD pattern of the gatifloxacin-Ba complex reveals a distinct alteration compared to pure gatifloxacin. The crystalline form of gatifloxacin (form-Y) has PXRD-peaks at 5.1, 6.2, 7.8, 9.1, 9.8, 10.4, 12.9, 13.6, 14.3, 17.3, 17.7, 18.3, 18.8, 19.6, 20.7, 21.1, 23.4, 23.9, 24.4, 25.4, 25.9, and 26.6 ± 0.2 degrees, which are consistent with experimental data (Table 4). (https://trea.com/information/crystalline-forms-of-gatifloxacin/patentgrant/7a18a46e-c8f3-45ca-aea1-d4dccf0bdec6, Accessed on 25th August 2025).

The diffraction peaks matched with ICDD PDF number 00-005-0448, corresponding to barite ($BaSO_4$) with an orthorhombic crystal structure. The PXRD pattern suggests the formation of a modified crystalline phase associated with the presence of Ba(II). These observations are consistent with possible structural modification following interaction between Ba(II) and gatifloxacin.

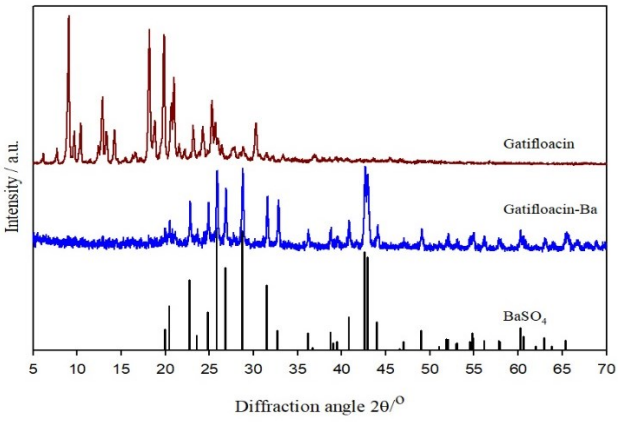
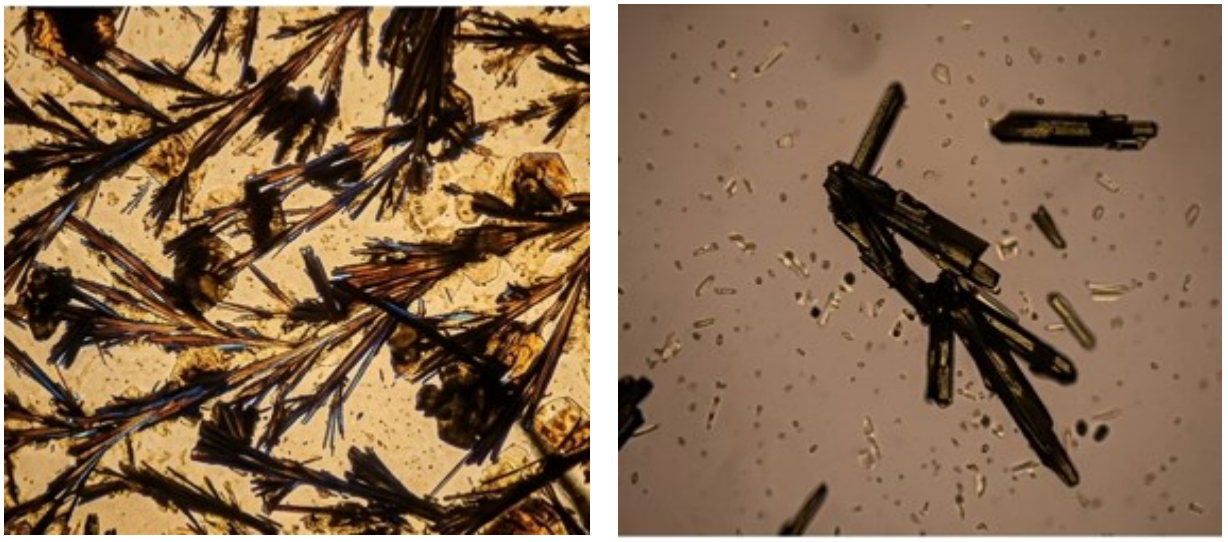


Figure 6. PXRD pattern of gatifloxacin-Ba complex.

Table 4. Characteristic 2θ peaks, observed crystalline phases, and structural interpretations for each drug-metal complex

Drug/ complex	Characteristic 2θ peaks (°)	Observed phase/structure
Gatifloxacin	5.1, 6.2, 7.8, 9.1, 9.8, 10.4, 12.9, 13.6, 14.3, 17.3–26.6	Crystalline (form-Y, consistent with literature)
Gatifloxacin-Mn	6.2, 7.9, 10.2, 13.8, 17.5, 18.7, 20.5, 23.5, 25.7	Mixed amorphous–crystalline (Mn incorporated, disrupted lattice)
Gatifloxacin-Ba	5.2, 7.0, 9.2, 14.0, 18.5, 21.0, 23.8, 26.5	Orthorhombic $BaSO_4$ phase (barite-like)

Partial loss of long-range order and presence of both crystalline and amorphous domains are indicated by the observed rise in background noise and the broadening of peaks in the complexes' diffractograms. This behavior is commonly observed in pharmaceutical solid dispersions and drug-metal coordination systems [34, 35]. It is significant that PXRD was only used as a qualitative tool for phase identification and crystallinity assessment. Since single-crystal X-ray diffraction data were not gathered, no thorough crystal structure solution or refinement was attempted. Pharmaceutical and coordination chemistry research are two areas where PXRD is widely used to confirm phase purity, lattice changes, and solid-state transitions [36-38].



(A) (B)

Figure 7. Trinocular microscopic images illustrating the crystal morphology of the synthesized metal–drug complexes. Distinct needle- and rod-shaped crystalline aggregates are observed for (A) Gatifloxacin–Mn(II) and (B) Gatifloxacin–Ba(II), indicating differences in crystal habit following complex formation.

Crystal habit observations

Microscopic examination under a trinocular microscope revealed that the synthesized complexes formed well-defined crystalline aggregates (Fig. 7).

Representative images of gatifloxacin-Mn, and gatifloxacin-Ba showed differences in morphology compared to the parent drugs. These morphological variations suggested significant interaction between drug molecules and metal ions, thereby justifying subsequent PXRD investigations. This analysis highlighted significant modifications in the crystalline framework of the investigated drugs upon metal incorporation. Gatifloxacin-Mn displayed a mixed amorphous–crystalline phase, whereas gatifloxacin–Ba exhibited a highly ordered orthorhombic lattice. These results are consistent with earlier studies that demonstrated the ability of divalent cations to disrupt or stabilize fluoroquinolone crystal lattices depending on their ionic radius and coordination geometry [39].

Antimicrobial activity

The antimicrobial activity of the synthesized gatifloxacin-metal complexes was evaluated against Gram-positive and Gram-negative pathogenic bacterial strains using the disc diffusion method (30 µg/disc). The inhibition zones were compared with a standard gatifloxacin disc (30 µg/disc). The results are summarized in Table 5.

Most complexes exhibited significant inhibitory effects against Gram-positive organisms, including *Streptococcus β-hemolyticus*, *Staphylococcus aureus*, *S. pyogenes*, *Bacillus subtilis* and *B. tropicus*. The Mn(II) complex demonstrated the highest activity, showing inhibition zones of 47.67 ± 0.67 mm and 41.0 ± 0.58 mm against *S. β-hemolyticus* and *S. pyogenes*, respectively. Similarly, Sr(II) and Co(II) complexes exhibited strong activity, particularly against *S. aureus* (46.0 ± 0.58 mm) and *B. tropicus* (50.0 ± 0.58 mm), surpassing the standard ciprofloxacin zone (39–42 mm). The Cu(II) complex also displayed broad-spectrum efficacy with inhibition zones up to 44.67 ± 0.33 mm. In contrast, Ni(II) and Fe(II) complexes showed lower activity, which may be attributed to reduced solubility or steric hindrance around the metal center that limits diffusion through the agar medium. The results in Table 6 suggest that coordination with transition metals may enhance the antimicrobial efficiency of gatifloxacin through chelation, facilitating drug penetration into bacterial membranes [40, 41]. Mn, Sr, Co, Cu, Pb, and Ag complexes of gatifloxacin show comparable or moderate to relatively strong activity to gatifloxacin. The pronounced activity of Cu(II), Pb(II), and Ag(I) complexes may arise from synergistic effects between gatifloxacin and metal ions, where the metal centers stabilize the quinolone's enolate oxygen, enhancing bacterial DNA-gyrase inhibition.

Silver's well-known antimicrobial effect related to Ag^+ ion release further contributes to its relatively higher activity [42]. Cu, Mg, Pb, Ag, and Sr complexes show higher zone of inhibition against standard gatifloxacin. Gatifloxacin shows consistent zones of ~39–46 mm, serving as an effective reference. Several complexes, notably Cu, Pb, Ag, Mn, and Sr, exhibit equal or relatively higher activity, suggesting enhanced chelation-based antimicrobial potential. Chelation-related effects on physicochemical properties may contribute to the observed differences in antibacterial activity. Some (e.g., Fe, Zn, Ni) show decreased activity, possibly attributed to low solubility or poor complexation.

Table 5. Antimicrobial screening of complexes formed by gatifloxacin and metal interactions against Gram-positive and Gram-negative pathogenic bacteria

-	Inhibition zones (mm)										
	Gram-positive pathogenic bacteria					Gram-negative pathogenic bacteria					
	(A)	*(B)*	*(C)*	*(D)*	*(E)*	*(F)*	*(G)*	*(H)*	*(I)*	*(J)*	*(K)*
Gat-30	37.33± 0.33	39.0 ± 1.0	41.67± 0.88	38.0 ± 0.58	39.67± 1.2	41.33 ±0.33	46.0± 0.58	40.67± 0.67	39.67± 0.67	39.0±0 .58	42.67± 1.33
Manganese-gatifloxacin complex	47.67± 0.67	24.67 ± 0.33	41.0±0. 58	21.33 ± 1.33	22.0± 1.0	36.67 ±0.33	34.33 ±1.33	12.33 ± 0.30	12.33 ±1.10	25.67± 0.33	28.0± 1.0
Strontium-gatifloxacin complex	41.67± 1.2	46.0 ± 0.58	44.33± 0.88	25.33 ± 1.2	39.67± 1.2	46.33 ±0.33	38.0± 1.0	44.0±1 .0	13.33 ± 0.23	28.67± 0.88	42.33± 0.33
Cobalt-gatifloxacin complex	45.67± 1.33	26.0 ± 1.0	45.0±0. 58	20.67 ± 0.33	21.67± 1.2	50.0± 0.58	41.0± 0.58	45.0±1 .0	13.33 ± 1.12	35.67± 0.88	41.0 ± 0.0
Calcium - gatifloxacin complex	43.33± 1.2	11.33 ± 1.33	28.33± 0.88	39.0 ± 0.58	24.67± 0.33	43.33 ±0.33	42.67 ±0.88	37.0±1 .0	11.33 ± 1.22	12.3 ± 1.33	45.0 ± 1.0
Nickel-gatifloxacin complex	44.33± 1.2	37.0 ± 0.58	12.67± 0.88	38.0 ± 1.15	28.0± 1.15	32.33 ±0.88	38.0± 0.58	36.67± 0.67	18.0±0 .58	10.23 ± 0.53	39.0 ± 1.0
Magnesium-gatifloxacin A complex	47.33± 0.88	15.33 ± 1.2	27.0±1. 0	39.0 ± 1.0	28.0± 1.15	14.33 ±0.67	42.67 ±0.67	45.33± 0.33	10.33 ± 0.3	24.33± 0.88	43.33± 0.33
Barium-gatifloxacin complex	42.67± 0.33	34.67 ± 0.88	43.67± 1.2	17.33 ± 0.33	32.0± 0.0	29.0 ±1.0	41.0± 0.58	42.0±0 .58	14.33 ± 0.35	38.0±0 .58	34.67 ± 1.2
Copper (II) - gatifloxacin complex	43.33± 0.67	41.67 ± 0.88	44.67± 0.33	28.0 ± 0.58	42.33± 0.88	43.33 ±1.2	10.33 ±0.88	10.33 ± 1.33	19.33± 0.33	38.0±0 .0	45.67± 0.88
Zinc - gatifloxacin complex	43.0± 0.0	19.0 ± 0.58	43.33± 0.88	26.0 ± 0.58	24.33± 1.33	29.67 ±0.33	29.0± 0.58	15.67± 0.67	15.33± 0.33	32.67± 1.33	26.0 ± 0.58
Iron (II) - gatifloxacin complex	41.33± 0.33	16.67 ± 1.2	10.33 ± 1.30	26.67 ± 0.67	25.33± 0.88	17.67 ±1.2	36.0± 1.0	10.33 ± 1.33	31.0± 0.58	31.33± 0.67	45.0 ± 0.0
Magnesium – gatifloxacin B complex	44.67± 1.33	34.33 ± 0.67	17.33± 0.88	30.0 ± 0.58	27.33± 0.88	37.33 ±1.2	42.0± 1.0	10.33 ± 1.33	38.67± 0.67	37.67± 0.88	47.33± 0.67
Lead - gatifloxacin complex	46.0±0. 58	33.33 ± 0.88	17.33± 0.88	30.0 ± 1.15	36.67± 0.67	34.67 ±0.88	39.33 ±0.88	10.33 ± 1.33	33.33± 0.33	24.67± 1.2	48.0 ± 1.0
Silver-gatifloxacin complex	37.67± 0.67	44.0 ± 0.58	12.33 ± 1.23	24.0 ± 0.58	33.67± 0.33	42.33 ±0.67	42.67± 1.2	10.33 ± 1.33	43.33± 0.33	47.33± 0.33	24.67 ± 1.2

Values are presented as mean inhibition zone diameters ((n=3). In each sample 30 μg/disc complex substance was applied and Gat-30 was the standard disc of gatifloxacin 30 µg/disc.

Table 6. Antimicrobial activity observed against Gram-positive bacteria of gatifloxacin-metal complexes.

Metal complex	Observations	Remarks
Manganese- gatifloxacin complex	Appreciable inhibition zones, especially *vs Streptococcus β-hemolyticus* (47.67 mm) and *S. pyogenes* (41.0 mm)	Mn complex shows broader inhibition profile.
Strontium- gatifloxacin complex	High activity, notably *vs S. aureus* (46 mm) and *Bacillus tropicus* (39.67 mm)	Sr enhances gatifloxacin's efficacy.
Cobalt- gatifloxacin complex	Strong effect on *Streptococcus β-hemolyticus (*45.67 mm), *Streptococcus pyogenes* (45 mm)	Cobalt complex exhibits good potency.
Calcium - gatifloxacin complex	Moderate to strong inhibition on *S. β-hemolyticus* (43.33 mm) and *Bacillus subtilis* (39 mm)	Calcium complex maintains good activity.
Nickel- gatifloxacin complex	High activity against *Streptococcus β-hemolyticus* (44.33 mm); lowest against *S. pyogenes* (12.67 mm)	Nickel reduces activity against most Gram-positive bacteria.
Magnesium- gatifloxacin A complex	Strong inhibition *vs S. β-hemolyticus* (47.33 mm), *Bacillus subtilis* (39 mm)	Magnesium complex retains broad efficacy.
Barium- gatifloxacin complex	Good inhibition, esp. *vs S. pyogenes* (43.67 mm)	Barium complex is active.
Copper (II) - gatifloxacin complex	Strong zones across many strains, e.g., *S. pyogenes* (44.67 mm)	Copper complex shows comperatively larger zone of inhibition.
Zinc - gatifloxacin complex	Good inhibition vs *S. β-hemolyticus* (47.33 mm), *Streptococcus pyogenes* (43 mm)	Zinc complex moderately effective.
Iron (II) - gatifloxacin complex	Weak to moderate, no inhibition against *S. pyogenes*.	Iron complex reduces drug efficacy.
Magnesium - gatifloxacin B complex	Good inhibition vs *S. β-hemolyticus* (44 mm)	Good Gram-positive performance.
Lead - gatifloxacin complex	Appreciable inhibition zones, *S. β-hemolyticus* (46 mm)	Lead complex surprisingly effective.
Silver- gatifloxacin complex	Very good activity against *S. aureus* (44 mm)	Silver complex shows enhanced activity.

The majority of the tested complexes demonstrated moderate to strong activity against Gram-negative bacteria (Table 7).

Table 7. Antimicrobial activity of gatifloxacin-metal complexes against Gram-negative bacteria

Metal complex	Observations	Remarks
Manganese- gatifloxacin complex	Low activity (12–36 mm range).	Less effective.
Strontium- gatifloxacin complex	Strong zones *vs Shigella dysenteriae (46.33 mm) and E. coli* (44 mm).	Dual-spectrum activity.
Cobalt- gatifloxacin complex	Strong zones *vs Shigella dysenteriae (50 mm) and E. coli* (45 mm).	Effective for both Gram classes.
Calcium - gatifloxacin complex	Strong against *S. dysenteriae* (43.33 mm).	Retains efficacy vs Gram-negative.
Nickel- gatifloxacin complex	Weak *vs S. abony* (18 mm).	Reduced effect on Gram-negative.
Magnesium- gatifloxacin A complex	Strong *vs E. coli* (45.33 mm) and *S. typhi* (43.33 mm).	Broader inhibition profile.
Barium- gatifloxacin complex	Active *vs E. coli* (42 mm).	Moderate overall.
Copper (II) - gatifloxacin complex	Strong *vs P. aeruginosa* (38 mm) and *S. typhi* (45.67 mm).	Among the most potent.
Zinc - gatifloxacin complex	Low activity (15–32 mm range).	Less effective.

Metal complex	Observations	Remarks
Iron (II) - gatifloxacin complex	Moderate *vs Salmonella typhi* (45 mm). Weak to moderate; inactive *vs* some strains.	Interferes with antibacterial action in most cases.
Magnesium - gatifloxacin B complex	High *vs S. typhi* (47.33 mm).	Broader Gram-negative inhibitor.
Lead - gatifloxacin complex	Strong *vs S. typhi* (48 mm).	Enhanced activity.
Silver- gatifloxacin complex	Very active *vs Salmonella abony* (43.33 mm) and *Pseudomonas aeruginosa* (47.33 mm).	Relatively strong activity, likely attributed to synergistic Ag^+ antimicrobial property.

The present study reveals that the antimicrobial activity of gatifloxacin is significantly influenced by metal complexation. Complexes with Cu(II), Pb(II), Ag(I), and Mn(II) ions exhibited relatively broader inhibitory activity within the tested panel. Meanwhile, Fe(II) and Ni(II) complexes were less effective, suggesting possible antagonistic interactions or stability issues. These findings suggest that such complexes may serve as promising candidates for further *in vivo* pharmacological studies and potential development of next-generation metal–antibiotic formulations [43, 44].

Statistical analysis

Mean inhibition zone diameters (mm) derived from triplicate measurements were used to express antimicrobial activity. The metal complexes and free gatifloxacin were qualitatively compared using the mean values. No inferential statistical analysis was done because of the study's preliminary nature and the small number of triplicates. As a result, antimicrobial efficacy was evaluated using observed variations in inhibition zone widths, a method frequently used in preliminary screening investigations of metal-drug complexes with the goal of detecting structure-activity patterns.

Limitation statement

Since elemental and magnetic tests were not carried out, the structural interpretations mostly relied on FT-IR, DSC, and PXRD evaluations. As such, the coordination mechanisms are to be considered as proposed. Similarly, the antimicrobial data were obtained *via* disc diffusion assays, providing qualitative comparisons; further studies involving MIC, MBC, and more statistical analyses are required to reach definitive conclusions.

CONCLUSION

Gatifloxacin complexes with several transition metal ions, alkaline-earth metal ions and Ag ion were synthesized and comparatively evaluated using FT-IR, DSC, PXRD, and microscopic techniques. Spectroscopic thermal analysis proposed the formation of bidentate metal-ligand complexes with possible coordination environments. The complexes showed larger inhibition zones, particularly Cu(II), Co(II), Pb(II), Ag(I), Sr(II), and Mn(II) derivatives, against tested bacterial strains, supporting further investigation of metal complexation approaches. These findings provide a foundation for further exploration of metal-based fluoroquinolone derivatives in combating multidrug-resistant pathogens. The differences observed in antimicrobial activity could be linked to modifications in physicochemical properties that occur after metal complexation, which may include changes in lipophilicity and interactions with membranes. Additionally, the potential synergistic effects arising from the coordinated metal ions should be acknowledged; however, these mechanisms were not explicitly assessed in this study and necessitate further experimental validation. These findings suggest a potential role of metal complexation in enhancing the activity by preliminary *in vitro* observations. PXRD analysis indicated that the Mn(II) complex displays a combination of amorphous and crystalline phases, while the Ba(II) complex has a stable orthorhombic structure akin to barite. X-ray diffraction demonstrated a degree of lattice disruption and a mixed amorphous–crystalline characteristic for the Mn(II) complex, in contrast to the Ba(II) complex, which resulted in a clearly defined orthorhombic crystalline phase. Overall, this work demonstrates that metal–gatifloxacin complexes represent promising candidates for developing new antimicrobial agents, especially in the context of combating multidrug-resistant pathogens. Future studies focusing on *in vitro* MIC/MBC and *in vivo* pharmacological evaluation, toxicity profiling, and structural optimization could further advance their potential as antimicrobial therapeutics.

Acknowledgement: *The authors gratefully acknowledge the Centre for Advanced Research in Sciences (CARS), University of Dhaka, Bangladesh, and the Laboratory of Pharmaceutical Microbiology, International Islamic University Chittagong, Bangladesh, for providing essential support, resources, and infrastructural facilities necessary for carrying out this research.*

Conflict of interest: *There are no conflicts to declare.*

Financing: *The work was carried out without financing.*

Contributions of authors*: Conception and design, or design of the research; or the acquisition, analysis, or interpretation of data: MAS, MZS, MAR, HAS. Drafting the manuscript or revising it critically for important intellectual content: MAS, MZS, MMM, MAR, HAS. Final approval of the version to be published: MAR. Agreement to be accountable for all aspects of the work in ensuring that questions related to the accuracy or integrity of any part of the work are appropriately investigated and resolved: MAR.*

REFERENCES

1. World Health Organization, Antimicrobial Resistance: A Manual for Developing National Action Plans, World Health Organization, Geneva, 2016, p. 1.
2. C. L. Ventola, *Pharm. Ther.*, **40**, 277 (2015).
3. G. D. Wright, *Nat. Prod. Rep.*, **34**, 694 (2017). DOI: 10.1039/C7NP00019G
4. Z. H. Chohan, C. T. Supuran, A. Scozzafava, *J. Enzyme Inhib. Med. Chem.*, **20**, 303 (2005). DOI: 10.1080/14756360310001624948
5. C. A. Akinremi, J. A. Obaleye, S. A. Amolegbe, J. F. Adediji, M. O. Bamigboye, *Int. J. Med. Biomed. Res.*, **1**, 24 (2012). DOI: 10.14194/ijmbr.115
6. V. E. Anderson N. Osheroff, *Curr. Pharm. Des.*, **7**, 337 (2001). DOI: 10.2174/1381612013398013
7. P. C. Appelbaum P. A. Hunter, *Int. J. Antimicrob. Agents*, **16**, 5 (2000). DOI: 10.1016/S0924-8579(00)00192-8
8. J. Anane, E. Owusu, G. Rivera,
9. D. Bandyopadhyay, *Int. J. Mol. Sci.*, **25**, 2263 (2024). DOI: 10.3390/ijms25042263
10. M. Ferreira, P. Gameiro, *Microorganisms*, **9**, 1506 (2021). DOI: 10.3390/microorganisms9071506
11. S. A. Sadeek, W. H. El-Shwiniy, *J. Mol. Struct.*, **977**, 243 (2010). DOI: 10.1016/j. molstruc.2010.05.041
12. I. Turel, *Coord. Chem. Rev.*, **232**, 27 (2002). DOI: 10.1016/S0010-8545(02)00027-9
13. A. Solanki, M. H. Sadhu, S. B. Kumar, P. Mitra, *J. Mol. Struct.*, **1076**, 475 (2014). DOI: 10.1016/j.molstruc.2014.07.082
14. N. Chavain, C. Biot, *Curr. Med. Chem.*, **17**, 2729 (2010). DOI: 10.2174/092986710791859306
15. N. Sultana, A. Naz, M. S. Arayne, M. A. Mesaik, *J. Mol. Struct.*, **969**, 17 (2010). DOI: 10.1016/j.molstruc.2010.01.036
16. Z. Q. Li, F. J. Wu, Y. Gong, C. W. Hu, Y. H. Zhang, M. Y. Gan, *Chin. J. Chem.*, **25**, 1809 (2007). DOI: 10.1002/cjoc.200790334
17. N. Dave, H. Bhatt, *Asian J. Chem. Sci.*, **10**, 98 (2021). DOI: 10.9734/ajocs/2021/v10i419109
18. H. A. Jawad, I. O. Alfatlawi, E. A. Alyasiry, S. Kadhim, *Afr. J. Biomed. Res.*, **28** (2025). DOI: 10.53555/AJBR.v28i3S.7766
19. M. K. Kumari, Spectroscopic Techniques in Pharmaceutical Analysis, in Pharmaceutical Analysis: A Comprehensive Guide, 2025, p. 154.
20. D. Dorniani, M. Z. Hussein, A. U. Kura, S. Fakurazi, A. H. Shaari, Z. Ahmad, *Int. J. Mol. Sci.*, **14**, 23639 (2013).
21. M. Ahmad, Ziaullah, N. U. Islam, M. Ali, S. Khan, *Chem. Afr.*, **7**, 4139 (2024). DOI: 10.1007/s42250-024-01059-1
22. P. Kumari, V. Lather, S. Khatri, P. Ahlawat, H. Sehrawat, S. P. Khatkar, V. B. Taxak, R. Kumar, *RSC Adv.*, **12**, 35827 (2022). DOI: 10.1039/D2RA05796D
23. S. P. Fricker, *Dalton Trans.*, **43**, 4903 (2007). DOI: 10.1039/b705551j.
24. C. L. Domínguez-Delgado, E. Fuentes-Prado, J. J. Escobar-Chávez, G. Vidal-Romero, I. M. Rodríguez-Cruz, R. Díaz-Torres, Chitosan and Pluronic® F-127*:* Pharmaceutical Applications, in: Encyclopedia of Biomedical Polymers and Polymeric Biomaterials, **11**, 1513 (2016). DOI: 10.1081/E-EBPP-120050057
25. J. M. Blondeau, *Surv. Ophthalmol.*, **49**, S73 (2004). DOI: 10.1016/j.survophthal.2004.01.005
26. S. Khatri, M. Kumar, R. Kumar, *Ann. Rom. Soc. Cell Biol.*, **25**, 396 (2021).
27. A. M. Shalash, H. I. Abu Ali, *Chem. Cent. J.*, **11**, 40 (2017). DOI: 10.1186/s13065-017-0268-2.
28. M. Z. Sultan, M. A. Sayeed, M. M. Masud, M. A. Rashid, *Indian J. Chem.*, **64**, 1089 (2025). DOI: 10.56042/ijc.v64i11.23368
29. S. Inouye, T. Takizawa, H. Yamaguchi, *J. Antimicrob. Chemother.*, **47**, 565 (2001). DOI: 10.1093/jac/47.5.565
30. N. E. El-Gamel, M. A. Zayed, *Spectrochim. Acta A Mol. Biomol. Spectrosc.*, **82**, 414 (2011). DOI: 10.1016/j.saa.2011.07.072
31. T. A. Hajam, H. Saleem, M. Syed Ali Padusha, K. K. Mohammed Ameen, *Polycycl. Aromat. Compd.*, **42**, 6662 (2022).
32. W. A. Zordok, *Spectrochim. Acta A Mol. Biomol. Spectrosc.*, **129**, 519 (2014).
33. M. S. Refat, *Spectrochim. Acta A Mol. Biomol. Spectrosc.*, **68**(5), 1393 (2007). DOI: 10.1016/j.saa.2006.12.078
34. S. S. Patil *et al*., Crystalline Forms of Gatifloxacin, US Pat., US20060270705A1 (2006).
35. H. G. Brittain, *Profiles Drug Subst., Excipients Relat. Methodol.*, **30**, 271 (2003). DOI: 10.1016/S0099-5428(03)30010-3
36. B. C. Hancock, G. Zografi, *J. Pharm. Sci.*, **86**, 1 (1997). DOI: 10.1021/js9601896

37. S. Gates-Rector, T. Blanton, *Powder Diffr.*, **34**, 352 (2019). DOI: 10.1017/S0885715619000812
38. B. D. Cullity, S. R. Stock, Elements of X-Ray Diffraction, 3rd edn., Prentice Hall, 2001.
39. P. Khadka, J. Ro, H. Kim, I. Kim, J. T. Kim, H. Kim *et al.*, *Asian J. Pharm. Sci.*, **9**, 304 (2014). DOI: 10.1016/j.ajps.2014.05.005
40. P. J. Sadler, *J. Inorg. Biochem.*, **67**, 4 (1997).
41. S. Khabnadideh, R. Mohamadi, A. Farrothroz, *Bioorg. Med. Chem.*, **13**(17), 2863 (2003).
42. A. N. Mustapha, N. P. Ndahi, B. B. Paul, M. B. Fugu, *J. Chem. Pharm. Res.*, **6**, 588 (2014).
43. N. Raman, A. Kulandaisamy, C. Thangaraja, P. Manisankar, S. Viswanathan, C. Vedhi, *Transition Met. Chem.*, **29**, 129 (2004). DOI: 10.1023/B:TMCH.0000019409.50574.0a
44. A. Rusu, G. Hancu, S. Imre, *Adv. Pharm. Bull.*, **8**, 181 (2018). DOI: 10.15171/apb.2018.022.
45. K. Ajay, *Int. J. Life Sci.*, **6**, 446 (2018).